euspen's 24th International Conference & Exhibition, Dublin, IE, June 2024
www.euspen.eu

Machining characteristics of Ti6Al4V in electrochemical machining (ECM) and hybrid laser-ECM

Muhammad Hazak Arshad[1,2], Krishna Kumar Saxena[1,2], Dominiek Reynaerts[1,2,*]

[1]*Micro- & Precision Engineering Group (MPE), Manufacturing Processes and Systems (MaPS), Dept. of Mech. Eng., KU Leuven, Leuven, Belgium*
[2]*Member Flanders Make (https://www.flandersmake.be/nl), Leuven, Belgium*

[*] *dominiek.reynaerts@kuleuven.be*

Abstract

The titanium alloy (Ti6Al4V) exhibits lightweight, high strength, biocompatibility, thermal stability at extreme temperatures and corrosion resistance which makes it attractive for a wide range of industries. However, these properties contribute to its low machinability which is further complicated for microscale features. Additive manufacturing (AM) offers good flexibility and accuracy but the high thermal load generates internal pores and alters the material properties making it unsuitable for high-end applications. Electrochemical machining (ECM) can anodically dissolve materials independent of their hardness and preserve their properties, but the multiphase and passivating nature of Ti6Al4V limits its performance. Aggressive reagents or glycol-based electrolytes are needed for improved EC-dissolution but are harmful or have low current efficiency, respectively. Hybrid laser-ECM (LECM) was recently developed to circumvent these issues and improve the material processing window of ECM in aqueous neutral salt electrolytes by coaxially applying laser assistance simultaneously in the machining zone.
Therefore, in this work the machining characteristics of Ti6Al4V in ECM and LECM are presented to evaluate the processing improvement with laser assistance in terms of removal localisation, material removal rate (M.R.R.) and surface quality (Sa). With the growing interest in flexible manufacturing, samples manufactured with selective laser melting (SLM) were machined along with rolled samples to also investigate the influence of porosity and microstructure generated by SLM on EC/Laser-EC dissolution.

Keywords: Electrochemical machining (ECM), Hybrid laser-ECM (LECM), hybrid manufacturing, micromachining.

1. Introduction

Titanium alloys like Ti6Al4V are key industry materials with applications in automotive, aerospace, biomedical, etc. due to their lightweight, corrosion resistance, high strength, high hardness, biocompatibility and thermal stability at extreme temperatures. However, its high strength and low thermal conductivity create machining challenges [1], which are further magnified for microscale features. Additive manufacturing (AM) is gaining interest for net shaping Ti6Al4V parts due to its good flexibility and accuracy [2]. However, the high thermal loads in AM generate pores and change the material properties, which limit high-end aerospace and biomedical applications.

Electrochemical machining (ECM) can anodically dissolve materials independent of their hardness in the presence of an electrolyte and voltage source [3]. The athermal nature of ECM ensures good surface integrity and preservation of material properties which makes it suitablefor high-end applications. Unfortunately, the multiphase and highly passivating nature of Ti6Al4V also complicates EC-dissolution in aqueous neutral salt electrolytes, resulting in inhomogenous dissolution [4], [5]. Aggressive acid and base additives are needed to overcome the passivation barrier which are harmful for both the users and machine tool. A safer approach is to use ethylene glycol-based electrolytes to homogenously process Ti6Al4V, since the absence of water mitigates passive layer formation [6]. However, these electrolytes suffer from low current efficiency which limits their industrial scalability and the research is still on-going. Recently, a hybrid machining approach i.e. hybrid laser-electrochemical machining (LECM) was developed to circumvent the passivation and multiphase EC-dissolution challenges [7]. LECM can simultaneously apply the laser and ECM process energies at the machining zone, and the process parameters are controlled to avoid electrolyte boiling. Hence, the laser improves ECM material processing windows and capabilities by increasing the local current density, weakening the passive layer and enhancing reaction kinetics, making it promising for processing Ti6Al4V. Since LECM is being development for difficult-to-cut materials, it is necessary to evaluate its machining performance and process-material interactions using advanced materials currently facing machining challenges.

Therefore, the processing of Ti6Al4V is investigated for the first time with LECM using design of experiments (DOE) alongside ECM towards assessing and optimising the LECM machining performance. Furthermore, with the growing interest of AM for net shaping Ti6Al4V and subsequently, postprocessing it to improve surface integrity [8], as-built samples prepared through selective laser melting (SLM) [9] were used alongside monolythic rolled samples. The machining characteristics of the material and ECM/LECM were evaluated in terms of material removal rate (M.R.R.), surface roughness (*Sa*) and removal localisation, to correlate the LECM processing improvement as well as influence of material microstructure and process parameters. The results indicated that material processing improved with LECM whereas, the SLMed samples performed poorly owing to internal porosities and a less reactive martensitic microstructure.

2. Experimental

The experiments were conducted on the in-house built hybrid-LECM setup. The details of the process and experiments are provided in the following subsections.

2.1. Process principle

In the LECM process shown in Fig. 1, the laser and electrolyte flow coaxially through the tubular electrode for simultaneous application of the process energies in the machining zone. The tubular tool (1.2 mm O.D. and 0.65 mm I.D.) which has an inner quartz capillary serves as both the multimodal waveguide and ECM tool. The nanosecond (ns) pulsed green laser (532 nm) has the least absorption in water (α = 0.0045 /m) so, it mainly heats the workpiece surface. This focuses the least resistance current path towards the laser exit area and changes the ring shaped tool dependent current density distribution towards the center. These synergised effects lead to an increase in local current density which enhances transpassive dissolution, passivation weakening and removal localisation. The passive layer weakening is achieved via dissolution of material underneath the porous layer, which leads to layer flake-off with the electrolyte flow. Furthermore, the higher local current density with LECM provides sufficient energy to dissolve less reactive phases making it a promising technique for passivating multiphase materials like Ti6Al4V.

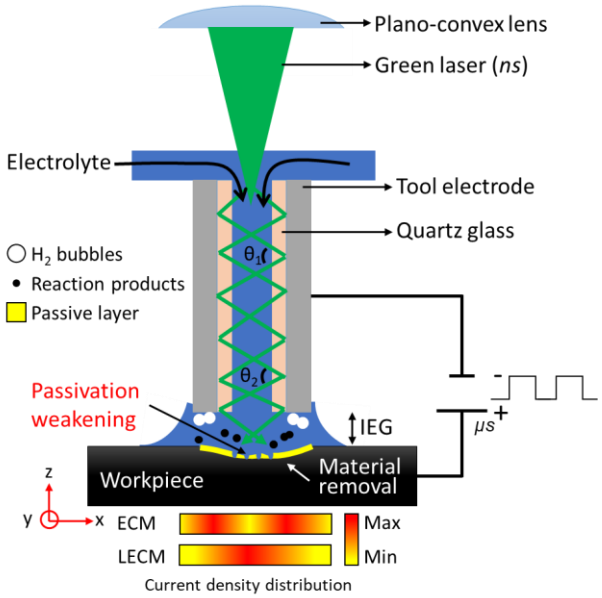

Figure 1. The process scheme of LECM process.

2.2. Experiments

The experiments were performed in 20% aq. sodium nitrate electrolyte (112 mS/cm at 20 °C) using a multi-level factorial design using parameters based on preliminary experiments (Table 1). The other fixed parameters were: 80 µm interelectrode gap (IEG), 0.35 mL/s electrolyte flow rate, 10 µs voltage pulse width at 50% duty cycle. The parameters for the LECM process mode were: 25 µJ laser pulse energy, 35 ns pulse width, 150 kHz pulse frequency. Two channels of 4 mm length were machined for each parameters combination on the 20x20x5 mm SLMed and rolled Ti6Al4V samples leading to a total of 48 experimental runs.

Table 1. Design of experiments (DOE) with factors and levels.

Parameter	Levels	Level values		
Material	2	Rolled	SLMed	-
Process Mode	2	ECM	LECM	-
Voltage	3	25 V	35 V	45 V
Feed rate	2	0.03 mm/s	0.06 mm/s	-

The scanning electron microscopy (SEM) images of the microstructure of etched samples are shown in Fig. 2. The rolled sample exhibited equiaxed α phase with β phase at grain boundaries whereas, the SLMed sample had an acicular α' martensitic microstructure due to rapid cooling during SLM. The SLMed sample had a density of 4.388 g/cm^3 (99.63% of rolled sample) due to the process generated porosity, which was also verified by the 0.16% defect volume measured by a CT scan.

After ultrasonic cleaning in deionized water for 20 mins, the samples were weighed on a Mettler Toledo® XS105 microbalance to calculate the M.R.R. and the channel dimensions were measured using the Keyence® VHS6000 digital microscope. The *Sa* was measured using Sensofar S neox with a 300x300 µm section area in the highest current density region (10x objective, L-filter 25µm, S-filter 2.5µm, ISO 16610-61). The DOE analysis was performed using Minitab®. Six measurements were performed for each experimental run.

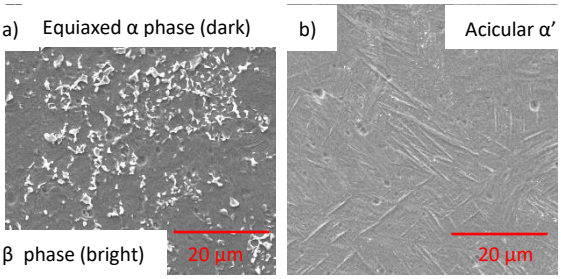

Figure 2. Microstructure of a) rolled and b) SLMed Ti6Al4V samples.

3. Results and discussion

The machining characteristics on the basis of M.R.R., *Sa* and channel dimensions measurements were used to investigate the influence of material, process parameters and processing improvement with LECM. These machining characteristics are discussed in the following subsections using the DOE analysis with main effects plots (error bars are standard errors of fitted means) and Pareto charts of the standardized effects with significance level at 95% of confidence level.

3.1. Material removal rate (M.R.R.)

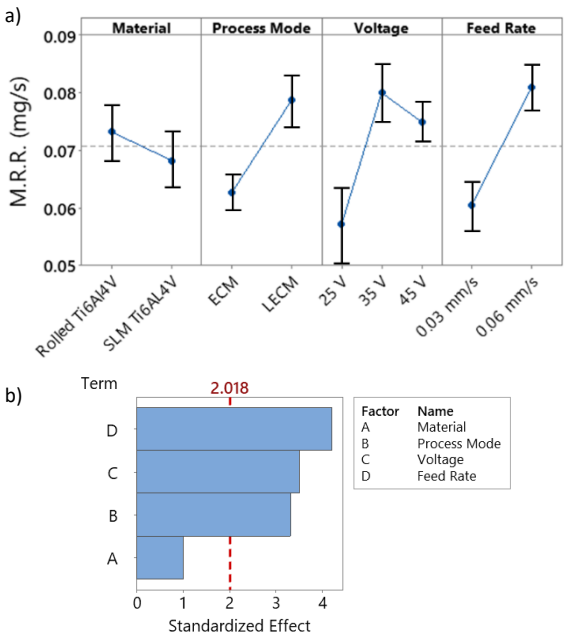

Figure 3. a) Main effects plots and b) Pareto chart for M.R.R.

The main effects plot (Fig. 3a) indicates that the material processing was 6.7% slower with the SLMed sample. This can be attributed to the less reactive martensitic phase. However, it seems that it did not have a significant influence on M.R.R.

(Fig. 3b) since the material composition was the same. The M.R.R. increased by 25% with LECM as the laser helped in increasing transpassive dissolution and passivation weakening, which was also a significant parameter. The influence of increasing voltage was peculiar since M.R.R. first increased (40%) and then decreased (6%). The increase in M.R.R. was expected since a higher voltage provides more current for material dissolution. The M.R.R. decrease at 45 V was probably due to increased joule heating which led to increase in re-passivation at the used electrolyte flow rate [10]. This heating was further increased during LECM at 45 V with possible boiling of small electrolyte packets. Feed rate was the most significant parameter and the M.R.R. increased by 34% with the higher feed rate of 0.06 mm/s. Faster scanning means that the gap is more clear due to less accumulation of by-products in the IEG, leading to improved material processing.

3.2. Surface roughness (Sa)

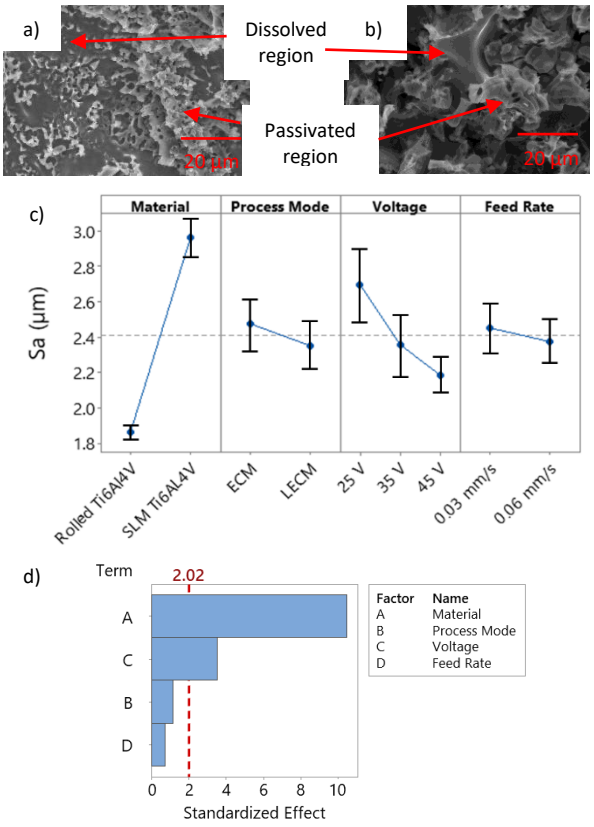

Figure 4. Machined surface (35 V and 0.06 mm/s) of a) rolled and b) SLMed samples. c) Main effects plots and d) Pareto chart for *Sa*.

The machined surfaces had distinct randomly distributed passivated and dissolved regions (Fig. 4a,b). *Sa* was selected to estimate the influence of LECM and process parameters in weakening the passivation to smoothen the surface. For the case of surface roughness, material was the most significant parameter (Fig. 4d) as the SLMed sample had a 59% higher *Sa* (Fig. 4c). This was due to the inherent rough surface (6.9±0.4 µm) of the as-built SLMed sample which was ~8 times higher than the rolled sample (0.86±0.03 µm). The porosity and less reactive microstructure possibly also played a role. The surface quality improved with both LECM and increasing voltage, which was expected since the surface asperities level out at higher current densities due to improved formation of the polishing salt film. The *Sa* was less sensitive (66%) to LECM than voltage because the primary dissolution mechanism is still anodic dissolution in LECM. Laser helps improve surface quality through increase in local current density which weakens passivation and enhances uniform multiphase dissolution at a particular voltage level [7]. Whereas, increasing the voltage level has a larger influence as it significantly increases the current density which accelerates the polishing salt film formation. The *Sa* was least sensitive to feed rate since the relatively cleaner gap conditions at 0.06 mm/s may have slightly improved the uniformity of the current density distribution across the workpiece surface.

3.3. Channel dimensions

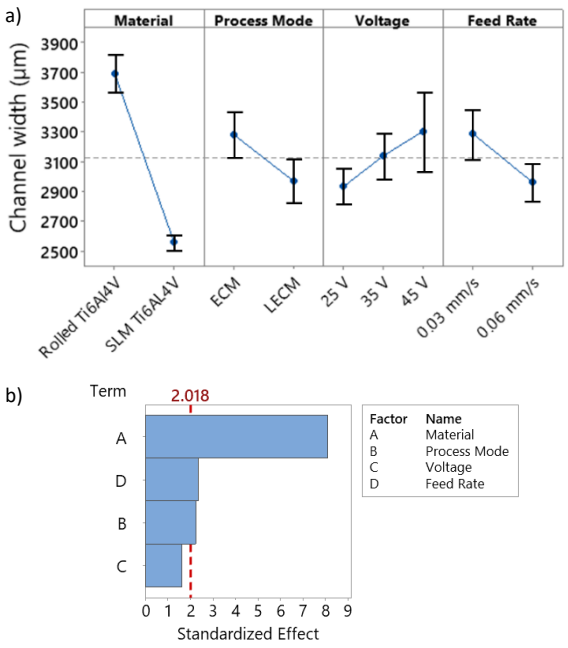

Figure 5. a) Main effects plots and b) Pareto chart for channel width.

The channel width and depth measurements represent removal localisation with LECM, process parameters and sample material.

The channels on rolled samples were 44% wider than SLMed samples at the same parameters (Fig. 5a), making material the most influential parameter (Fig. 5b). The passivation on the channel walls of the less reactive martensitic phase SLMed samples possibly created an overall higher resistance barrier which reduced lateral dissolution. The internal porosity also had an influence which is discussed with channel depth analysis. The tool feed rate and process mode had a similar degree of influence. At the higher feed rate the relatively uniform current density distribution reduces stray lateral dissolution and the less residence time reduces overall material removal, contributing to 11% width decrease. With LECM, the stray lateral dissolution reduces (9.5%) due to the change in current density distribution from ring shape to the laser exit area which reduces stray current around the tool [7]. Additionally, since the laser is directed towards the depth direction, the increase in local current density primarily weakens the passive layer on the channel basal surface and wall passivation is largely unaffected, which helps in removal localisation. This makes LECM especially suitable for processing passivating materials. Interestingly, the channel width was least sensitive to voltage and increased (~7%) with voltage, since a higher voltage leads to increased stray current around the tool.

Similar to channel width, the depth was most sensitive to material with 45% deeper channels on SLMed samples than rolled samples (Fig. 6). The higher channel depth and lower width of SLMed samples are largely influenced by the manufacturing process induced internal keyhole porosity. As the material dissolution front progresses in the depth direction, the surface passivation layer on the rolled sample always exists

which hinders material removal. Whereas, in the SLMed sample as the dissolution front proceeds, the internal pores possibly get exposed which reveal fresh unpassivated surfaces thatbecome preferential dissolution sites. These fresh surfaces on the basal surface promote dissolution in the depth direction due to incomplete surface passivation as shown in Fig. 7. LECM further accelerates this mechanism due to improved passivation weakening on the basal surface. This finding may provide the manufacturing community a new approach for engineering the part to posses high porosity at locations that require postprocessing after AM to facilitate easier material removal and precision. Apart from this, feed rate also had a significant influence as the depth decreased by 39% with higher feed rate owing to the decreased residence time. With voltage increase to 35 V the depth increased by 44% due to higher current density but decreased by 6% upon further increase to 45 V due to increased heating and re-passivation which are amplified by LECM [10]. This decrease at 45 V was also reflected in the decrease in M.R.R. since dissolution retardation and depth decrease by increased re-passivation had a larger influence than increase in channel width. Furthermore, LECM increased channel depth due to passivation weakening (Fig. 7) and removal localisation however, compared to other parameters its influence was less significant as the laser improves EC-processing at a particular voltage level.

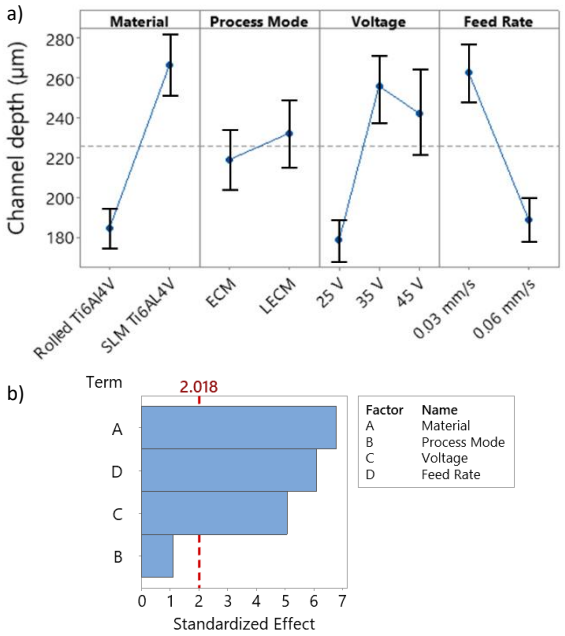

Figure 6. a) Main effects plots and b) Pareto chart for channel depth.

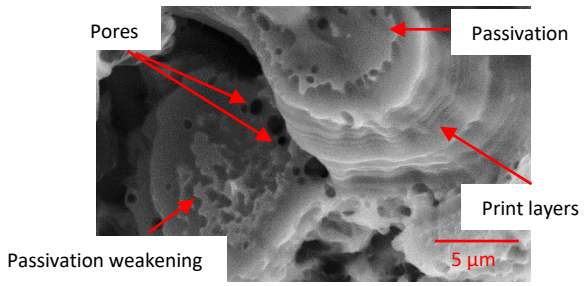

Figure 7. Processed surface of SLMed sample with LECM at 35 V and 0.06 mm/s with exposed pores.

4. Conclusion

The machining characteristics of Ti6Al4V samples in ECM and LECM produced by rolling and SLM were investigated in this study. The different manufacturing process dependent microstructure has a lower influence on the removal behaviour governed by first principles (M.R.R.) due to the same material composition. However, the combined effect of microstructure and internal porositiy considerably affects the surface topography and shape morphology. The less reactive martensitic phase of SLMed samples decreases material removal and stray dissolution whereas, the internal porosities expose unpassivated sites on the basal surface that preferentially dissolve to increase channel depth. This is interesting for manufacturing engineers to optimise the AM part design for postprocessing. The synegistics effects of LECM improved material processing for both samples and it performed better on all the criteria studied as long as the adverse heating effects are avoided by controlling the process parameters. These aspects make LECM promising for machining passivating multiphase materials and will be explored in the future on more 'difficult-to-cut' and 'difficult-to-dissolve' materials as means to improve surface integrity and machining localisation.

Acknowledgement

This work was supported by the FWO senior research project fundamental research (G099420N).

References

[1] F. Klocke, M. Zeis, A. Klink, and D. Veselovac, "Experimental research on the Electrochemical Machining of modern titanium- and nickel-based alloys for aero engine components," *Procedia CIRP*, vol. 6, pp. 368–372, 2013.

[2] B. Vrancken, L. Thijs, J. P. Kruth, and J. Van Humbeeck, "Heat treatment of Ti6Al4V produced by Selective Laser Melting: Microstructure and mechanical properties," *J. Alloys Compd.*, vol. 541, pp. 177–185, 2012.

[3] K. K. Saxena, J. Qian, and D. Reynaerts, "A review on process capabilities of electrochemical micromachining and its hybrid variants," *Int. J. Mach. Tools Manuf.*, vol. 127, no. July 2017, pp. 28–56, 2018, doi: 10.1016/j.ijmachtools.2018.01.004.

[4] A. Speidel, J. Mitchell-Smith, I. Bisterov, and A. T. Clare, "Oscillatory behaviour in the electrochemical jet processing of titanium," *J. Mater. Process. Technol.*, vol. 273, no. May, p. 116264, 2019, doi: 10.1016/j.jmatprotec.2019.116264.

[5] S. Hizume and W. Natsu, "Problems and solutions in scanning electrochemical machining of titanium alloys," *Procedia CIRP*, vol. 95, pp. 712–716, 2020, doi: 10.1016/j.procir.2020.02.285.

[6] W. Liu, Z. Luo, and M. Kunieda, "Electrolyte jet machining of Ti1023 titanium alloy using NaCl ethylene glycol-based electrolyte," *J. Mater. Process. Technol.*, vol. 283, no. April, p. 116731, 2020, doi: 10.1016/j.jmatprotec.2020.116731.

[7] K. K. Saxena, J. Qian, and D. Reynaerts, "A tool-based hybrid laser-electrochemical micromachining process: Experimental investigations and synergistic effects," *Int. J. Mach. Tools Manuf.*, vol. 155, no. May, p. 103569, 2020.

[8] H. Zeidler and F. Böttger-Hiller, "Plasma-Electrolytic Polishing as a Post-Processing Technology for Additively Manufactured Parts," *Chemie-Ingenieur-Technik*, vol. 94, no. 7, pp. 1024–1029, 2022, doi: 10.1002/cite.202200043.

[9] J. Metelkova, C. De Formanoir, H. Haitjema, A. Witvrouw, W. Pfleging, and B. Van Hooreweder, "Elevated edges of metal parts produced by laser powder bed fusion : characterization and post-process correction," *Proc. Spec. Interes. Gr. Meet. Adv. Precis. Addit. Manuf.*, no. September, pp. 1–4, 2019.

[10] M. H. Arshad, M. Wu, K. K. Saxena, and D. Reynaerts, "Analysis of passivation during ECM and hybrid laser-ECM through automated current pulse analysis," in *18th International Symposium on Electrochemical Machining Technology*, 2022, pp. 123–130.